Water wave scattering by a submerged thick wall with a gap

Mridula Kanoria

Physics and Applied Mathematics Unit, Indian Statistical Institute, 203, B.T. Road, Calcutta 700 0035, India

Received 19 May 1998; accepted 7 September 1998

Abstract

This article is concerned with scattering of surface water waves by a thick submerged rectangular wall with a gap in finite depth water. Multi-term Galerkin approximations involving ultraspherical Gegenbauer polynomials for solving first kind integral equations are utilised in the mathematical analysis to obtain very accurate numerical estimates for the reflection coefficient, which are depicted graphically against the wave number.

Keywords: Linear theory; Wave scattering; Thick barrier; Galerkin approximation; Ultraspherical Gegenbauer polynomials; Reflection coefficient

1. Introduction

The problem of water wave scattering by thin vertical barriers of various configurations and its modification when another identical barrier is introduced in water of uniform finite depth, have been studied extensively in the literature assuming linear theory (cf. Packman and Williams [1], Losada et al. [2], Mandal and Dolai [3], Kanoria and Mandal [4], Banerjea et al [5], Das et al. [6]) by employing various mathematical techniques. When the obstacle is in the form of a thick vertical barrier with rectangular cross-section present in water of uniform finite depth, the corresponding water wave scattering problems for normal incidence of a wave train have been investigated earlier by Mei and Black [7]. They considered surface piercing and bottom standing thick vertical barriers and used variational formulations as the basis for numerical computations of the reflection and the transmission coefficients, and obtained an accuracy within one percent for the numerical results. Bai [8] studied the problem of oblique wave scattering by a surface piercing long cylinder in finite depth water by employing finite element technique and presented graphically the numerical results for the reflection and transmission coefficients when the cylinder is of rectangular cross-section. Liu and Wu [9] used the method of matched asymptotic expansion to study the problem of oblique wave scattering by a thin as well as thick rectangular wall with a narrow gap in water of finite depth. However, their study is limited to long wave case only since they approximated the Helmoltz's equation by Laplace's equation for obtaining the linear solution. When the gap is not narrow, the method of matched asymptotic expansion to handle the associated wave scattering problem is no longer suitable. Recently, Mandal and Kanoria [14] and Kanoria et al. [15] considered the problems of oblique and normal wave scattering by thick barriers respectively, wherein the barriers have four types of configurations such as surface-piercing or bottom standing thick barrier or a submerged block, or a thick wall with a gap. They used multi-term Galerkin approximation method involving ultraspherical Gegenbauer polynomials for solving first kind integral equations arising in the mathematical analysis to obtain very accurate numerical estimates for the reflection coefficient.

The present problem is concerned with scattering of a train of surface water waves obliquely or normally incident on a submerged thick vertical wall of rectangular cross-section with a gap in water of uniform finite depth. Using the symmetry in the geometry, the boundary value problem describing the physical situation is split into two separate problems involving symmetric and antisymmetric parts of the potential function. Appropriate eigenfunction expansion of each of these potentials in different regions, followed by a matching process across the vertical line through the right corner points of the gap, produce an integral equation for the unknown derivatives of the symmetric and antisymmetric potential functions along the horizontal direction. Also, for each case of the symmetric and antisymmetric potential function a real quantity related to the reflection and transmission coefficients is defined which is expressed in terms of an integral involving this unknown derivative across the gaps. Solutions of two integral equations ultimately provide the reflection and transmission coefficients. The two integral equations are solved here by appropriate multi-term Galerkin approximations involving ultraspherical Gegenbauer

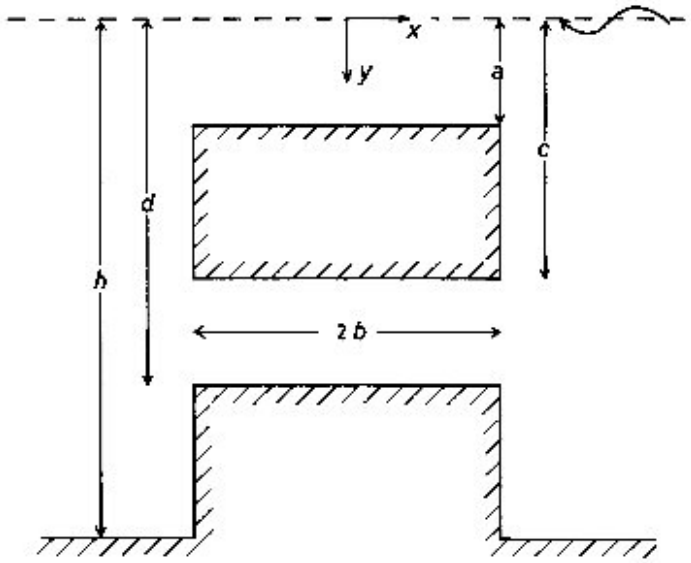

Fig. 1. Sketch of the problem.

polynomials, an idea originally suggested by Porter (cf. Evans and Fernyhough [10]).

The numerical estimates for the reflection coefficient are obtained with a six figure accuracy by choosing only four terms in the aforesaid multi-term expansions, and are depicted graphically against the wave number. It is observed that in contrast to the case of wall with a gap whose upper part is surface piercing, the reflection coefficient (for both oblique and normal incidence) has oscillatory behaviours as the wave number increases. This may be attributed to the interaction between the two ends of the submerged wall. Also, in the limiting case when the lower part of the wall is made very small and the distance between the bottom and the lower end of the upper part of the wall is also made small (but still greater than the small vertical length of the lower part) so that the submerged wall almost assumes the form of thick barrier standing at the bottom. The corresponding curves for the reflection coefficient almost coincide with those of Mandal and Kanoria [14] (oblique incidence) and Kanoria et al. [15] (normal incidence) which are also depicted here, for the same configuration.

Again, when the configuration assumes the form of submerged rectangular block over a rectangular bottom deformation of very small height, the reflection coefficient curves (for oblique as well as normal incidence), are seen to be qualitatively similar to the corresponding curves for a submerged block drawn earlier by Mandal and Kanoria [14] and Kanoria et al. [15] (also depicted here), although, these lie slightly above the curves for submerged block for some wave numbers and below for some other wave numbers. This may be attributed to the interaction between the two ends of the thick wall of very small height lying at the bottom.

Also, for very small values of the wave number the reflection coefficient in each case is seen to tend to zero, a result confirmed earlier for any obstacle by Martin and Dalrymple [12] and McIver [13] employing matched asymptotic expansions.

2. Formulation of the problem

We consider an obstacle in the form of a thick submerged vertical wall with a gap present in water of uniform finite depth h and choose y-axis vertically downwards along the line of symmetry of the thick barrier so that the obstacle occupies the region $-b \le x \le b, y \in L \equiv \{(a,c) + (d,h)\}$, where $0 < a < c < d < h$. Here a is the depth of the upper portion of the wall below the mean free surface, $2b$ is the thickness of the wall, $d - c$ is the gap length. This geometrical configuration of the wall is described in Fig. 1

We first consider the case of a train of surface water waves *obliquely* incident on the wall. The case of *normal* incidence can be dealt with after appropriate modifications in the analysis for oblique incidence. Under the assumption of linearised theory of water waves, the train of progressive surface water waves obliquely incident on the wall from very large distances on the right side is represented by the velocity potential $\mathrm{Re}\{\phi^{(1)\mathrm{inc}}(x,y)\mathrm{e}^{i(\nu z-\sigma t)}\}$, where

$$\phi^{(1)\mathrm{inc}}(x,y) = \frac{2\cosh k_0(h-y)\mathrm{e}^{-i\mu(x-b)}}{\cosh k_0 h} \tag{1}$$

k_0 is the unique real positive root of

$$k\tanh kh = K \tag{2}$$

with $K = \sigma^2/g$, σ being the circular frequency of the incoming wave train, g being the acceleration owing to gravity, $\mu = k_0 \cos\alpha$, $\nu = k_0 \sin\alpha$, α being the angle of incidence of the wave train. As a result of the symmetry in the geometry of the thick wall, the z-dependence can be eliminated by

assuming the velocity potential describing the motion in the fluid to be of the form $\mathrm{Re}\{\phi^{(1)}(x,y)e^{i(\nu z-\sigma t)}\}$. Henceforth the factor $e^{i(\nu z-\sigma t)}$ will always be suppressed. Then $\phi^{(1)}(x,y)$ satisfies

$$(\nabla^2-\nu^2)\phi^{(1)}=0 \qquad \text{in the fluid region} \tag{3}$$

$$K\phi^{(1)}+\phi^{(1)}_y=0 \qquad \text{on } y=0 \tag{4}$$

$$\phi^{(1)}_x=0 \qquad \text{on } x=\pm b, y\in L \tag{5}$$

$$r^{1/3}\nabla\phi^{(1)} \qquad \text{is bounded as } r\to 0 \tag{6}$$

where r is the distance from any submerged edge of the barrier,

$$\phi^{(1)}_y=0 \qquad \text{on } y=a,c,d,|x|<b \tag{7}$$

$$\phi^{(1)}_y=0 \qquad \text{on } y=h,|x|>b \tag{8}$$

$$\phi^{(1)}(x,y)\to\phi^{(1)\mathrm{inc}}(x,y)+R^{(1)}\phi^{(1)\mathrm{inc}}(-x,y) \qquad \text{as } x\to\infty$$

$$\phi^{(1)}(x,y)\to T^{(1)}\phi^{(1)\mathrm{inc}}(x,y) \qquad \text{as } x\to-\infty \tag{9}$$

where $R^{(1)}$ and $T^{(1)}$ denote respectively the reflection and transmission coefficients (complex) and are to be determined.

For normal incidence of the wave train, we will have $\alpha=0$ so that $\nu=0$, $\mu=k_0$ and the incident wave train is represented by $\mathrm{Re}\{\phi^{(0)\mathrm{inc}}(x,y)e^{-i\sigma t}\}$ where

$$\phi^{(0)\mathrm{inc}}(x,y)=\frac{2\cosh k_0(h-y)e^{-ik_0(x-b)}}{\cosh k_0 h} \tag{10}$$

The velocity potential describing the ensuing motion is denoted by $\mathrm{Re}\{\phi^{(0)\mathrm{inc}}(x,y)e^{-i\sigma t}\}$ where $\phi^{(0)}(x,y)$ satisfies Eq. (3) for $\nu=0$, the conditions (4)–(9) with superscript (1) replaced by (0) everywhere.

3. Method of solution

Due to geometrical symmetry, $\phi^{(1)}(x,y)$ can be split into symmetric and antisymmetric parts, $\phi^{(1)s}(x,y)$ and $\phi^{(1)a}(x,y)$ respectively, so that

$$\phi^{(1)}(x,y)=\phi^{(1)s}(x,y)+\phi^{(1)a}(x,y) \tag{11}$$

where

$$\phi^{(1)s}(x,y)=\phi^{(1)s}(-x,y), \qquad \phi^{(1)a}(-x,y)=-\phi^{(1)a}(x,y) \tag{12}$$

We need to consider only the region $x\geq 0$. Now $\phi^{s,a}(x,y)$ satisfy the Eqs. (3)–(8) together with

$$\phi^{(1)s}_x(0,y)=0, \quad \phi^{(1)a}(0,y)=0, \quad 0<y<h \tag{13}$$

Let the behaviour of $\phi^{(1)s,a}(x,y)$ as $x\to\infty$ be represented by

$$\phi^{(1)s,a}(x,y)\to\frac{\cosh k_0(h-y)}{\cosh k_0 h}[e^{-i\mu(x-b)}+R^{(1)s,a}e^{i\mu(x-b)}] \quad \text{as } x\to\infty \tag{14}$$

where $R^{(1)s,a}$ are constants, then by using (9), they are related to $R^{(1)}$ and $T^{(1)}$ by

$$R^{(1)},T^{(1)}=\frac{1}{2}(R^{(1)s}\pm R^{(1)a})e^{-2i\mu b} \tag{15}$$

The eigenfunction expansions of $\phi^{(1)s,a}(x,y)$ satisfying Eqs. (3)–(5), (7) and (8) for $x\geq 0$ is given below.

Region I ($x>b$, $0<y<h$):

$$\phi^{(1)s,a}(x,y)=\frac{\cosh k_0(h-y)}{\cosh k_0 h}[e^{-i\mu(x-b)}+R^{(1)s,a}e^{i\mu(x-b)}]+\sum_{n=1}^{\infty}A_n^{(1)s,a}\cos k_n(h-y)e^{-s_n(x-b)} \tag{16}$$

where $k_n(n=1,2,\ldots)$ are positive roots of

$$k\tan kh+K=0$$

and

$$s_n=(k_n^2+\nu^2)^{1/2} \tag{17}$$

For the case of normal incidence, the representation of $\phi^{(0)s,a}(x,y)$ can be obtained from Eqs. (16) by making $\alpha=0$ i.e. $\nu=0$, $\mu=k_0$ and replacing the superscript (1) by (0) and s_n by k_n.

Region II ($0<x<b$, $0<y<a$):

$$\begin{pmatrix}\phi^{(1)s}(x,y)\\ \phi^{(1)a}(x,y)\end{pmatrix}=\begin{pmatrix}B_0^{(1)s}\cos(\alpha_0^2-\nu^2)^{1/2}x\\ B_0^{(1)a}\sin(\alpha_0^2-\nu^2)^{1/2}x\end{pmatrix}\frac{\cosh\alpha_0(a-y)}{\cosh\alpha_0 a}+\sum_{n=1}^{\infty}\begin{pmatrix}B_n^{(1)s}\cosh t_n x\\ B_n^{(1)a}\sinh t_n x\end{pmatrix}\cos\alpha_n(a-y) \tag{18}$$

where $\pm\alpha_0$, $\pm i\alpha_n$ $(n=1,2,\ldots)$ are the roots of the equation

$$\alpha\tanh\alpha a=K$$

and

$$t_n=(\alpha_n^2+\nu^2)^{1/2}, n=1,2,\ldots \tag{19}$$

For the case of normal incidence, the representation of $\phi^{(0)s,a}(x,y)$ can be obtained form Eqs. (18) by making $\alpha=0$ and replacing the superscript (1) by (0) and t_n by α_n.

Region III ($0 < x < b, c < y < d$):

$$\begin{pmatrix}\phi^{(1)s}(x,y)\\ \phi^{(1)a}(x,y)\end{pmatrix} = \begin{pmatrix}C_0^{(1)s}\cosh \nu x\\ C_0^{(1)a}\sinh \nu x\end{pmatrix} + \sum_{n=1}^{\infty}\begin{pmatrix}C_n^{(1)s}\cosh \xi_n x\\ C_n^{(1)a}\sinh \xi_n x\end{pmatrix}\cos\frac{n\pi(d-y)}{d-c}$$

where

$$\xi_n = \left\{\left(\frac{n\pi}{d-c}\right)^2 + \nu^2\right\}^{1/2}, n = 1,2,\ldots \tag{20}$$

For the case of normal incidence, $\phi^{(0)s,a}$ are obtained from (20) by putting $\nu = 0$ and replacing the superscript (1) by (0) with the modification that there is no $C_0^{(0)s}$ and the first term in the expansion of $\phi^{(0)a}(x,y)$ is $C_0^{(0)a}x$.

Let us define

$$\phi_x^{(1)s,a}(b+0,y) = f^{(1)s,a}(y),\ 0 < y < h, \tag{21}$$

then

$$f^{(1)s,a}(y) = 0 \qquad \text{for } y \in L, \tag{22}$$

$$\phi_x^{(1)s,a}(b-0,y) = f^{(1)s,a}(y), \qquad 0 < y < a, c < y < d \tag{23}$$

and due to Eqs. (6)

$$\begin{aligned} f^{(1)s,a}(y) &= 0(|a-y|^{-1/3}) \qquad \text{as } y \to a-0\\ f^{(1)s,a}(y) &= 0(|y-c|^{-1/3}) \qquad \text{as } y \to c+0\\ f^{(1)s,a}(y) &= 0(|d-y|^{-1/3}) \qquad \text{as } y \to d-0 \end{aligned} \tag{24}$$

Use of Eqs. (16), (18) in (21) followed by Havelock's inversion formula produces, after noting Eqs. (22),

$$1 - R^{(1)s,a} = \frac{4ik_0\cosh k_0 h}{\mu\delta_0}\int_{\bar{L}} f^{(1)s,a}(y)\cosh k_0(h-y)\mathrm{d}y \tag{25}$$

with

$$\delta_0 = 2k_0h + \sinh 2k_0h, \bar{L} = (0,h) - L = (0,a) + (c,d)$$

$$A_n^{(1)s,a} = -\frac{4k_n}{s_n\delta_n}\int_{\bar{L}} f^{(1)s,a}(y)\cos k_n(h-y)\mathrm{d}y \tag{26}$$

with $\delta_n = 2k_nh + \sin 2k_nh$ $(n = 1,2,\ldots)$,

$$B_0^{(1)s,a} = \frac{4\alpha_0\cosh \alpha_0 a}{(\alpha_0^2+\nu^2)^{1/2}\gamma_0} \times\left(-\frac{1}{\sin(\alpha_0^2+\nu^2)^{1/2}b}, \frac{1}{\cos(\alpha_0^2+\nu^2)^{1/2}b}\right) \times\int_0^a f^{(1)s,a}(y)\cosh \alpha_0(a-y)\mathrm{d}y \tag{27}$$

with $\gamma_0 = 2\alpha_0 a + \sinh 2\alpha_0 a$

$$B_n^{(1)s,a} = \frac{4\alpha_n}{t_n\gamma_n}\left(\frac{1}{\sinh t_nb}, \frac{1}{\cosh t_nb}\right)\int_0^a f^{(1)s,a}(y) \times\cos \alpha_n(a-y)\mathrm{d}y$$

with

$$\gamma_n = 2\alpha_n a + \sin 2\alpha_n a\ (n = 1,2,\ldots) \tag{28}$$

Using Eqs. (20) in Eqs. (23) and taking Fourier cosine inversion we obtain

$$C_0^{(1)s,a} = \frac{1}{\nu(d-c)}\left(\frac{1}{\sinh \nu b}, \frac{1}{\cosh \nu b}\right)\int_c^d f^{(1)s,a}(y)\mathrm{d}y, \tag{29}$$

$$C_n^{(1)s,a} = \frac{2}{\xi_n(d-c)}\left(\frac{1}{\sinh \xi_n b}, \frac{1}{\cosh \xi_n b}\right) \times\int_c^d f^{(1)s,a}(y)\cos\frac{n\pi(d-y)}{d-c}\mathrm{d}y, \quad (n = 1,2,\ldots). \tag{30}$$

For the case of normal incidence, $f^{(0)s}(y)$ must satisfy

$$\int_c^d f^{(0)s}(y)\mathrm{d}y = 0, \tag{31}$$

and the constant $C_0^{(0)a}$ is given by

$$C_0^{(0)a} = \frac{1}{d-c}\int_c^d f^{(0)a}(y)\mathrm{d}y \tag{32}$$

The other constants (with superscript (0)) are obtained in terms of integrals involving $f^{(0)s,a}(y)$ with suitable modifications in the above relations Eqs. (25)–(30).

Now, matching of $\phi^{(1)s,a}(x,y)$ across the line $x = b$ through the right corner points of the gap produces

$$\phi^{(1)s,a}(b+0,y) = \phi^{(1)s,a}(b-0,y), y \in \bar{L} \tag{33}$$

which eventually produces the integral equations for $f^{(1)s,a}(y)$, $y \in \bar{L}$ in the form

$$\int_{\bar{L}} M^{(1)s,a}(y,u)F^{(1)s,a}(u)\mathrm{d}u = \frac{\cosh k_0(h-y)}{\cosh k_0h}, \quad y \in \bar{L} \tag{34}$$

where

$$F^{(1)s,a}(y) = \frac{4k_0\cosh^2 k_0h}{\mu\delta_0(1+R^{(1)s,a})}f^{(1)s,a}(y), \quad y \in \bar{L}. \tag{35}$$

$M^{(1)s,a}(y,u)$ are real and symmetric in y and u, and their expressions are given in Appendix A.

If we now define the constants $C^{(1)s,a}$ by

$$C^{(1)s,a} = -i\frac{1-R^{(1)s,a}}{1+R^{(1)s,a}}, \tag{36}$$

then Eqs. (25) produces, after using Eqs. (33),

$$\int_{\bar{L}} F^{(1)s,a}(y)\frac{\cosh k_0(h-y)}{\cosh k_0h}\mathrm{d}y = C^{(1)s,a}. \tag{37}$$

Table 1
Reflection coefficient $|R^{(1)}|$, $\alpha = 45°$

$a/h = 0.2$, $c/h = 0.4$, $d/h = 0.6$, $b/h = 1$

Kh	$N=0$	$N=1$	$N=2$	$N=3$	$N=4$	$N=5$
0.01	0.383943	0.381812	0.381797	0.381794	0.381794	0.381794
1.0	0.442127	0.443633	0.443648	0.443648	0.443648	0.443648
1.8	0.797051	0.798831	0.799157	0.799156	0.799156	0.799156

Table 2
Reflection coefficient $|R^{(0)}|$

$a/h = 0.2$, $c/h = 0.4$, $d/h = 0.6$, $b/h = 1$

Kh	$N=0$	$N=1$	$N=2$	$N=3$	$N=4$	$N=5$
0.01	0.477645	0.475608	0.475549	0.475546	0.475546	0.475546
1.0	0469505	0.457956	0.457619	0.457586	0.457582	0.457582
1.8	0.793569	0.793524	0.793230	0.793227	0.793226	0.793226

It is important to note that $F^{(1)s,a}(y)$ and $C^{(1)s,a}$ are all real quantities. Thus, if the integral Eq. (34) are solved, then these solutions can be utilised to obtain $C^{(1)s,a}$ from Eq. (37), which in turn produce the actual reflection and transmission coefficients $|R^{(1)}|$ and $|T^{(1)}|$ respectively by using

$$|R^{(1)}| = \frac{|1 + C^{(1)s}C^{(1)a}|}{\Delta}; \qquad |T^{(1)}| = \frac{|C^{(1)s} - C^{(1)a}|}{\Delta} \tag{38}$$

where

$$\Delta = \left\{1 + (C^{(1)a})^2 + (C^{(1)a})^2 + (C^{(1)s}C^{(1)a})^2\right\}^{1/2}, \tag{39}$$

the relations (38) being obtained from Eqs. (15) and (36).

To solve the integral Eqs. (34), we seek an approximation

$$F^{(1)s,a}(y) \approx \mathscr{F}^{(1)s,a}(y), \qquad y \in \bar{L} \tag{40}$$

where $\mathscr{F}^{(1)s,a}(y)$ will be expressed as multi-term Galerkin expansion in terms of suitable basis functions.

For the double interval $\bar{L} = (0,a) + (c,d)$, $\mathscr{F}^{(1)s,a}(y)$ are expressed as

$$\begin{aligned} \mathscr{F}^{(1)s,a}(y) &= \sum_{n=0}^{N} a_n^{(1)s,a} f^{(1)s,a}(y), \qquad 0 < y < a \\ \mathscr{F}^{(1)s,a}(y) &= \sum_{n=0}^{N} b_n^{(1)s,a} g^{(1)s,a}(y), \qquad c < y < d \end{aligned} \tag{41}$$

where the basis functions $f^{(1)s,a}(y)$ $(0 < y < a)$ and $g_n^{(1)s,a}(y)$ $(c < y < d)$ in Eq. (41) are given in Appendix C.

We substitute the expansion (41) in Eq. (34) multiply first by $f_m^{(1)s,a}$ and then by $g_m^{(1)s,a}(y)$ and integrate over $(0,a)$ and (c,d) respectively to obtain the two linear systems

$$\sum_{n=0}^{N} a_n^{(1)s,a}\begin{pmatrix} G_{mn}^{(1)s,a} \\ P_{mn}^{(1)s,a} \end{pmatrix} + \sum_{n=0}^{N} b_n^{(1)s,a}\begin{pmatrix} H_{mn}^{(1)s,a} \\ Q_{mn}^{(1)s,a} \end{pmatrix} = \begin{pmatrix} p_m^{(1)s,a} \\ q_m^{(1)s,a} \end{pmatrix}$$
$$m = 0, 1 \ldots N \tag{42}$$

where

$$G_{mn}^{(1)s,a} = \int_0^a \left\{\int_0^a M^{(1)s,a}(y,u) f_n^{(1)s,a}(u)\mathrm{d}u\right\} f_m^{(1)s,a}(y)\mathrm{d}y,$$

$$H_{mn}^{(1)s,a} = \int_0^a \left\{\int_c^d M^{(1)s,a}(y,u) f_n^{(1)s,a}(u)\mathrm{d}u\right\} f_m^{(1)s,a}(y)\mathrm{d}y,$$

$$P_{mn}^{(1)s,a} = \int_c^d \left\{\int_0^a M^{(1)s,a}(y,u) f_n^{(1)s,a}(u)\mathrm{d}u\right\} g_m^{(1)s,a}(y)\mathrm{d}y,$$

$$Q_{mn}^{(1)s,a} = \int_c^d \left\{\int_c^d M^{(1)s,a}(y,u) f_n^{(1)s,a}(u)\mathrm{d}u\right\} g_m^{(1)s,a}(y)\mathrm{d}y, \tag{43}$$

so that $H_{nm}^{(1)s,a} = P_{nm}^{(1)s,a}$, and

$$\begin{aligned} p_m^{(1)s,a} &= \int_0^a \frac{\cosh k_0(h-y)}{\cosh k_0 h} f_m^{(1)s,a}(y)\mathrm{d}y, \\ q_m^{(1)s,a} &= \int_c^d \frac{\cosh k_0(h-y)}{\cosh k_0 h} g_m^{(1)s,a}(y)\mathrm{d}y, \end{aligned} \tag{44}$$

The expressions in Eqs. (43) and Eqs. (44) can be simplified and these are given Appendix C.

Approximation to $C^{(1)s,a}$ in this case is obtained from Eq. (37) as

$$C^{(1)s,a} = \sum_{n=0}^{N} \{a_n^{(1)s,a} p_n^{(1)s,a} + b_n^{(1)s,a} q_n^{(1)s,a}\} \tag{45}$$

For the case of normal incidence, the supercript (1) is replaced by (0) and corresponding results for the kernel $M^{(0)s,a}(y,u)$, the basic functions $f_m^{(0)s,a}$, $g_m^{(0)s,a}$ and $G_{mn}^{(0)s,a}$, $H_{mn}^{(0)s,a}$, $P_{mn}^{(0)s,a}$, $Q_{mn}^{(0)s,a}$, $p_m^{(0)s,a}$, $q_m^{(0)s,a}$ are given in Appendix A, B and C respectively.

4. Numerical results and discussions

Since $|R^{(j)}|^2 + |T^{(j)}|^2 = 1$, $j = 0,1$, we confine our attention to the reflection coefficient $|R^{(j)}|$ $(j = 0,1)$ only. For this we have to compute the infinite series $G_{mn}^{(j)s,a}$, $H_{mn}^{(j)s,a}$, $P_{mn}^{(j)s,a}$ and $Q_{mn}^{(j)s,a}$, $(j = 0,1)$ of the form described in Appendix C. These series are computed by truncation. A six figure accuracy is achieved by taking two hundred terms in each series. The accuracy can be further increased by following a numerical procedure suggested by Porter and Evans [11]. This is not pursued here.

A representative set of these numerical estimates for $|R^{(1)}|$ and $|R^{(0)}|$ are tabulated in Tables 1 and 2 respectively, taking some particular values of a/h, b/h, c/h, d/h, $Kh = 0.01$, 1.0, 1.8 and $\alpha = 45°$ (for $|R^{(1)}|$). It is observed that the computed results for the reflection coefficient converge very rapidly with N, and for $N = 4$ an accuracy of almost six figures is achieved. For other geometries and other values of the wave numbers, very accurate estimates (six figures) for $|R^{(j)}|$ $(j = 0,1)$ are obtained and these are illustrated by plotting curves for $|R^{(j)}|$ $(j = 0,1)$ against the wave number Kh. The reflection coefficient is depicted graphically against Kh in Fig. 2, $a/h = 0.2$, $c/h = 0.4$, $d/h = 0.6$, $b/h = 1$, and for $\alpha = 0°$, 30°,

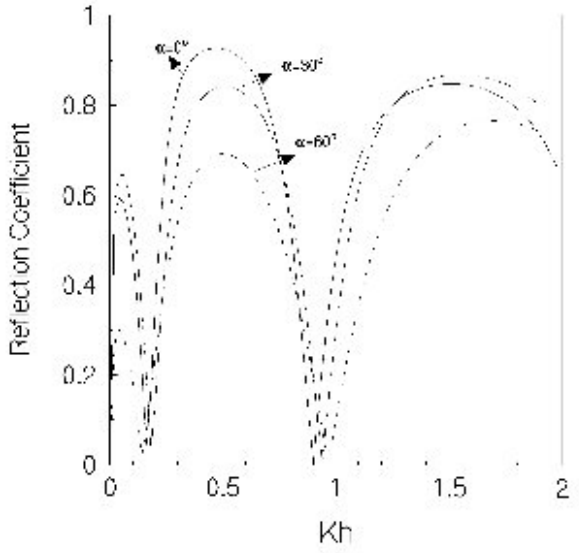

Fig. 2. Reflection coefficient versus wave number, $a/h = 0.2$, $c/h = 0.4$, $d/h = 0.6$.

60°. It is observed that the reflection coefficient decreases as α increases for a fixed wave number, and for fixed α, it oscillates and its zeros occur at certain wave numbers. The oscillatory behaviour is attributed due to interaction between the ends of the submerged wall. This is in contrast with the results for a thick wall with a gap, whose upper part is surface piercing. In that case the reflection coefficient as a function of wave number steadily increases with Kh from zero (at $Kh \to 0$) to unity (as $Kh \to \infty$).

To ascertain the effect of wall thickness, in Fig. 3, $|R^{(1)}|$ is plotted against Kh by taking $a/h = 0.2$, $c/h = 0.4$, $d/h = 0.6$, $\alpha = 45°$ for $b/h = 0.01$, 0.1, 1.0, 2.0. It is observed that the number of zeros of $|R^{(1)}|$ increases as the thickness increases. It is also seen from Fig. 3 that when the wall is comparatively thin ($b/h = 0.01$), $|R^{(1)}|$ first increases and then

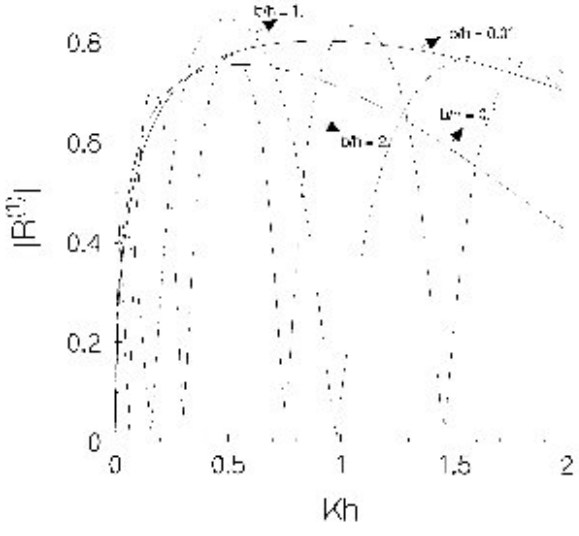

Fig. 3. Reflection coefficient versus wave number, $a/h = 0.2$, $c/h = 0.4$, $d/h = 0.6$, $\alpha = 45°$.

decreases asymptotically to zero with the increase of wave number. The same behaviour is also seen for $|R^{(0)}|$, which is not illustrated here. This is the usual behaviour for infinitely thin barrier. As thickness increases, $|R^{(1)}|$ starts fluctuating and the fluctuation increases as the thickness of the wall increases further. The same behaviour of $|R^{(0)}|$ is also observed, although $|R^{(0)}|$ is not depicted here. This oscillatory behaviour of the reflection coefficient is due to interaction between the two ends of the thick wall.

Now, in the limiting case when the lower part of the wall is made very small ($d/h = 0.999$), and the distance between the bottom and the lower end of the upper part of the wall is also made very small ($c/h = 0.99$), so that the submerged wall with a gap almost assumes the form of a bottom standing thick barrier, the corresponding curves for the reflection coefficient against the wave numbers are plotted in Figs. 4 and 5 for $\alpha = 45°$ ($a/h = 0.5$) and $\alpha = 0°$ ($a/h = 0.5$) respectively. It is seen that the curve in Fig. 4 almost coincides with the one given by Mandal and Kanoria [14], also plotted in the same figure. Similarly, in Fig. 5 the curve obtained coincides with the curve of Kanoria et al. [15], also plotted in the same figure. These provides some partial checks on the correctness of the numerical method adopted here.

Again, when the vertical length of the lower part of the wall is made very small, the configuration assumes the form of a submerged rectangular block over a rectangular bottom deformation of very small height. The result for a submerged thick rectangular block have been obtained recently by Mandal and Kanoria [14] for oblique incidence and by Kanoria et al. [15] for normal incidence. In Figs. 6 and 7 $|R^{(j)}|$ ($j = 0,1$) are depicted against Kh for $\alpha = 45°$ and 0°, and by taking $a/h = 0.2$, $c/h = 0.4$, $d/h = 0.99$, $b/h = 1.0$ (i.e. the vertical length of the lower part of the wall is very small) in both figures, respectively. In this case the reflection coefficients for a submerged wall whose lower part is very small in height and a submerged block of the same dimension as the upper part of the submerged wall, are also similar except that they do not exactly coincide although being quite near to each other. The small difference is perhaps due to the interaction of waves between the two ends of the lower part of the wall which still lies at the bottom and is at a considerable distance from the upper part.

It may be noted that the long wave limit of the reflection coefficient is seen to be zero in Figs. 2–7. This provides a partial check on the correctness of the numerical method utilised here. The long wave limit, zero, of the reflection coefficient for any obstacle has earlier been confirmed by Martin and Dalrymple [12] and McIver [13] by using matched asymptotic expansions for normal incidence.

5. Conclusion

The method of multi-term Galerkin approximations in

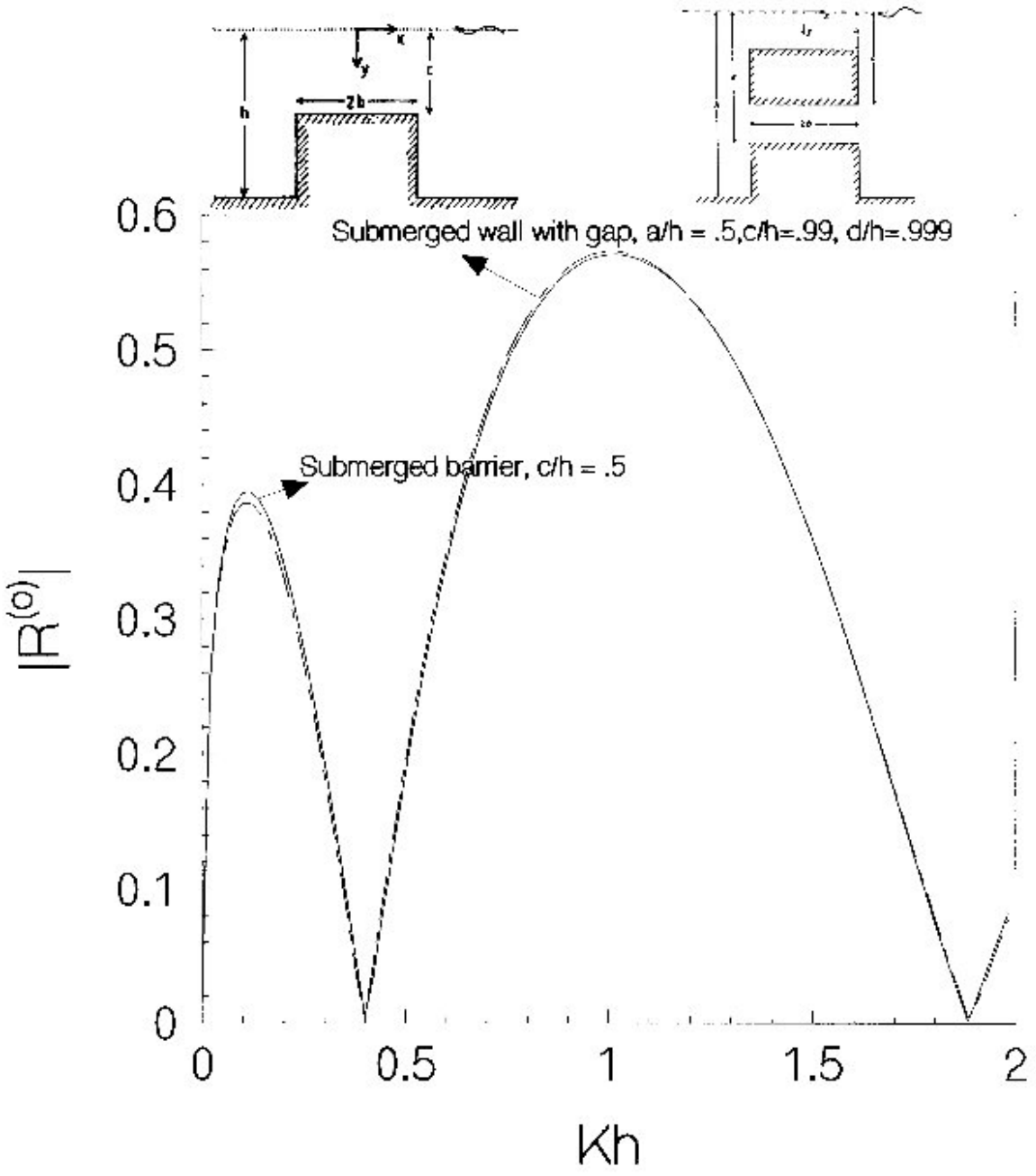

Fig. 5. Reflection coefficient versus wave number, $b/h = 1$.

The expression for $M^{(0)s}(y,u)$ is obtained from (A.1) by putting $\nu = 0$, $\mu = k_0$. Similarly $M^{(0)a}(y,u)$ can be obtained.

For $y,u \in (c,d)$

$$M^{(1)s}(y,u) = \frac{\mu\delta_0}{k_0\cosh^2 k_0 h}\left[\sum_{n=1}^{\infty}\left\{\frac{k_n\cos k_n(h-y)\cos k_n(h-u)}{s_n\delta_n} + \frac{1}{2(d-c)}\frac{\coth\xi_n b}{\xi_n}\cos\frac{n\pi(d-y)}{d-c}\cos\frac{n\pi(d-u)}{d-c}\right\} + \frac{1}{4(d-c)}\frac{\coth\nu b}{\nu}\right] \quad \text{(A.2)}$$

The expression for $M^{(1)a}(y,u)$ is obtained by replacing "coth" by "tanh". The expression for $M^{(0)s}(y,u)$ is obtained from Eqs. (A.2) by putting $\nu = 0$, $\mu = k_0$ and deleting the term $[\coth\nu b]/4(d-c)\nu$ is the square bracket. Similarly $M^{(0)a}(y,u)$ is obtained by deleting the term $[\tanh\nu b]/4(d-c)\nu$ in the square bracket of $M^{(1)a}(y,u)$.

For $y \in (0,a), u \in (c,d)$ and $y \in (c,d), u \in (0,a)$

$$M^{(1)s,a}(y,u) = \frac{\mu\delta_0}{k_0\cosh^2 k_0 h}\sum_{n=1}^{\infty}\frac{k_n\cos k_n(h-y)\cos k_n(h-u)}{s_n\delta_n} \quad \text{(A.3)}$$

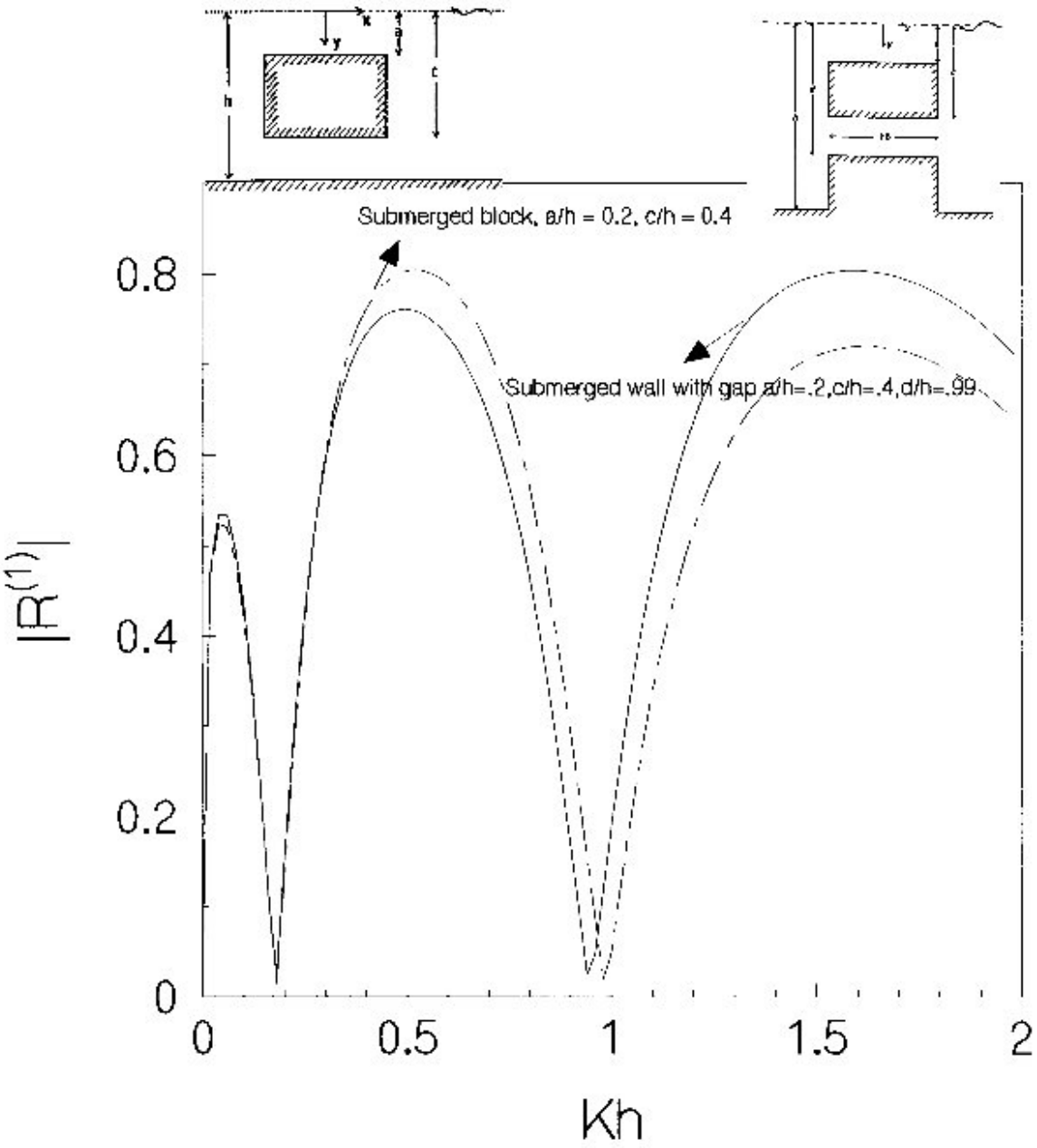

Fig. 6. Reflection coefficient versus wave number, $b/h = 1$, $\alpha = 45°$.

The expression for $M^{(0)s,a}(y,u)$ are obtained from (A.3) by putting $\alpha = 0$.

Appendix B. Basis functions

For $y \in (0,a)$:

In this case we have to consider the free surface condition and the behaviour $F^{(j)s,a}(y) \sim (a-y)^{-1/3}$, $j = 0, 1$, as $y \to a - 0$ derived by considering the flow field near the corner point (b,a). Thus $F^{(j)s,a}(y) \equiv F(y), j = 0, 1$, satisfies

$$KF(y) + F'(y) = 0 \qquad \text{on } y = 0, \tag{B.1}$$

$$F(y) \sim (a-y)^{-1/3} \qquad \text{as } y \to a - 0 \tag{B.2}$$

If we introduce

$$\hat{F}(y) = F(y) - K\int_0^a F(u)\mathrm{d}u, \qquad 0 < y < a \tag{B.3}$$

then

$$\hat{F}'(y) = 0 \qquad \text{on } y = 0, \tag{B.4}$$

$$\hat{F}(y) \sim (a-y)^{-1/3} \qquad \text{as } y \to a - 0. \tag{B.5}$$

The condition (B.4) shows that $\hat{F}(y)$ can be continued as an even function of y into $(-a,0)$. Thus, because of the condition (B.4), $(a^2 - y^2)^{1/3}\hat{F}(y)$ can be expanded in $(0,a)$ as a complete set of even ultraspherical Gegenbauer

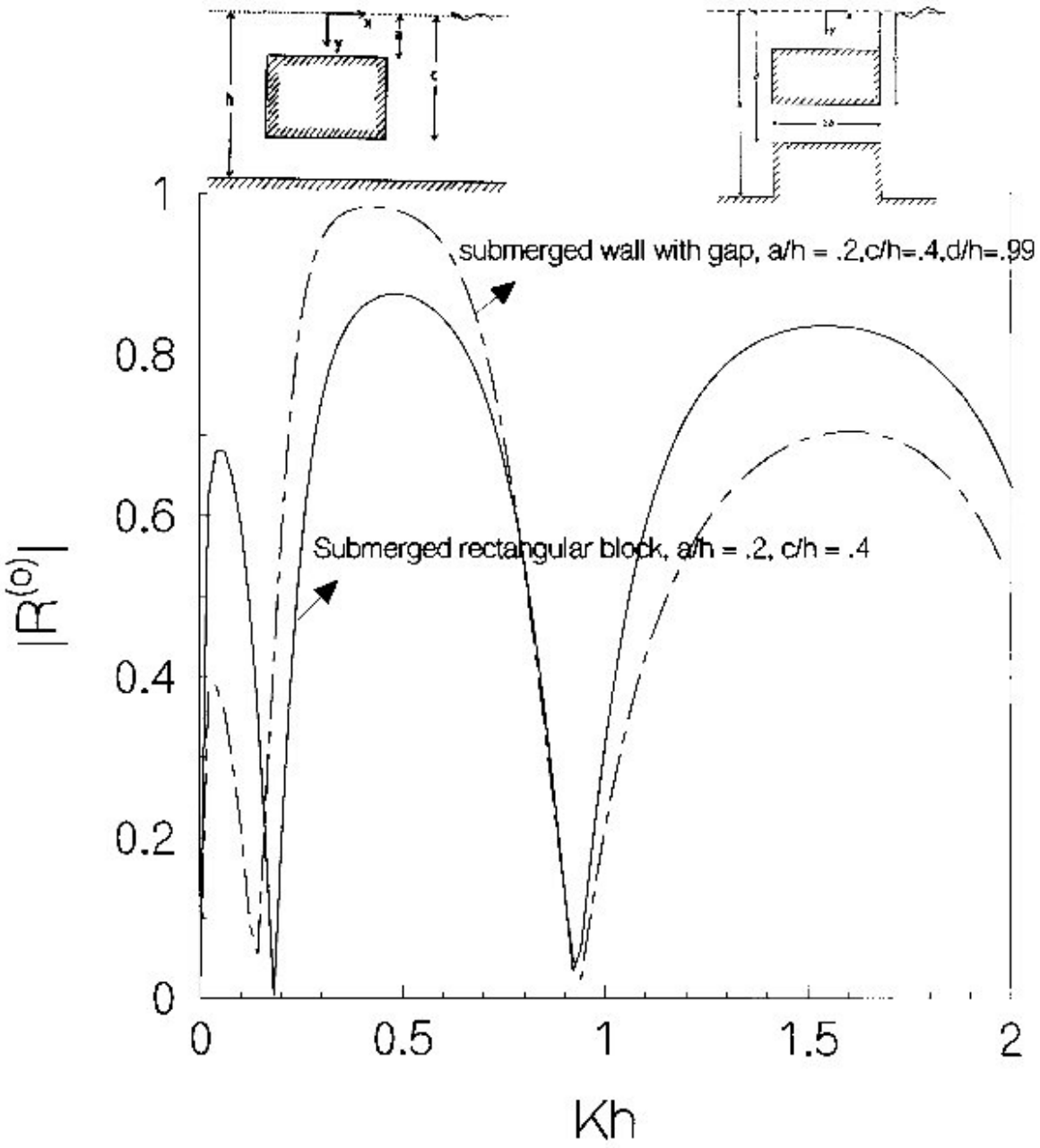

Fig. 7. Reflection coefficient versus wave number, $b/h = 1$.

polynomials $C_{2m}^{1/6}(y/a)$. Thus in this case the basis functions for $F^{(1)s,a}(y)\left(F^{(0)s,a}(y)\right)$ are found to be

$$f_m^{(1)s,a}(y)\left(f_m^{(0)s,a}(y)\right) = f_m(y) = -\frac{\mathrm{d}}{\mathrm{d}y}\left[\mathrm{e}^{-Ky}\int_0^a \mathrm{e}^{Kt}\hat{f}_m(t)\mathrm{d}t\right]$$

$$0 < y < a \tag{B.6}$$

where $\hat{f}_m(y)$ is chosen as

$$\hat{f}_m(y) = \frac{2^{7/6}\Gamma(1/6)(2m)!}{\pi\Gamma(2m+1/3)a^{1/3}(a^2-y^2)^{1/3}}C_{2m}^{1/6}(y/a) \tag{B.7}$$

For $y \in (c,d)$, we have to consider only the behaviours $F^{(1)s,a}(y)(F^{(0)s,a}(y)) \sim (y-c)^{-1/3}$ as $y \to c+0$ and $F^{(1)s,a}(y)\left(F^{(0)s,a}(y)\right) \sim (d-y)^{-1/3}$ as $y \to d-0$, and full set $C_m^{1/6}((2y-c-d)/(d-c))$ of ultraspherical Gegenbauer polynomials are used for expansion of $\{(y-c)(d-y)\}^{1/3}F^{(1)s,a}(y)$ in (c,d). Thus we choose

$$g_m^{(1)s,a}(y) = \frac{2^{1/6}\Gamma(1/6)m!}{\pi\Gamma(m+1/3)\left(\frac{d-c}{2}\right)^{1/3}\{(y-c)(d-y)\}^{1/3}} \times C_m^{1/6}\left(\frac{2y-c-d}{d-c}\right), \quad c < y < d \tag{B.8}$$

For $F^{(0)s,a}(y)$, we observe that $F^{(0)s}(y)$ satisfies the additional conditions (see Eq. (31))

$$\int_c^d F^{(0)s}(y)\mathrm{d}y = 0 \tag{B.9}$$

Noting again the result

$$\int_c^d \frac{1}{([d-c]/2)^{1/3}\{(y-c)(d-y)\}^{1/3}} C_n^{1/6}\left(\frac{2y-d-c}{d-c}\right)\mathrm{d}y = \int_{-1}^{1}(1-t^2)^{-1/3}C_n^{1/6}(t)\mathrm{d}t = 0 \quad \text{for } n>0 \tag{B.10}$$

We observe that the basis functions $F^{(0)s}(y)(c<y<d)$ are given by

$$g_m^{(0)s}(y) = g_{m+1}^{(1)s}(y), \qquad m = 0,1,\ldots N \tag{B.11}$$

while the basis functions for $F^{(0)a}(y)(c<y<d)$ are given by

$$g_m^{(0)a} = g_m^{(1)a}(y) \qquad m = 0,1,2,\ldots N \tag{B.12}$$

Appendix C

Expressions for $G_{mn}^{(j)s,a}, H_{mn}^{(j)s,a}, P_{mn}^{(j)s,a}, Q_{mn}^{(j)s,a}, p_m^{(j)}, q_m^{(j)}$, $j = 0, 1$.

For $\bar{L} = (0,a)+(c,d)$

$$G_{mn}^{(1)s} = \frac{\mu\delta_0}{k_0\cosh^2 k_0 h}\left[4(-1)^{n+m}\sum_{r=1}^{\infty}\left(\frac{k_r\cos^2 k_r h}{s_r\delta_r}\frac{J_{2n+1/6}(k_r a)J_{2n+1/6}(k_r a)}{(k_r a)^{1/3}} + \frac{\alpha_r}{t_r\gamma_r}\coth(t_r b)\cos^2\alpha_r a\frac{J_{2n+1/6}(\alpha_r a)J_{2m+1/6}(\alpha_r a)}{(\alpha_r a)^{1/3}}\right)\right.$$
$$\left. - \frac{\alpha_0}{\gamma_0}\frac{\cot\left\{\left(\alpha_0^2-\nu^2\right)^{1/2}b\right\}}{\left(\alpha_0^2-\nu^2\right)^{1/2}}\cosh^2\alpha_0 a\frac{I_{2n+1/6}(\alpha_0 a)I_{2m+1/6}(\alpha_0 a)}{(\alpha_0 a)^{1/3}}\right] \tag{C.1}$$

$G_{mn}^{(1)a}$ is obtained by replacing ''coth'' by ''tanh'' and '' − cot'' by ''tan'' in Eqs. (C.1).

$G_{mn}^{(0)s,a}$ are obtained from (C.1) by putting $\alpha = 0$ ($\nu = 0$, $\mu = k_0$).

$$H_{mn}^{(1)s,a} = \frac{4\mu\delta_0}{k_0\cosh^2 k_0 h}\sum_{r=1}^{\infty}\frac{k_r\cos k_r h}{s_r\delta_r}\begin{pmatrix}(-1)^{n/2}\cos k_r\left(h-\dfrac{c+d}{2}\right)\\ (-1)^{\frac{n-1}{2}}\sin k_r\left(h-\dfrac{c+d}{2}\right)\end{pmatrix}\times\frac{J_{2m+1/6}(k_r a)J_{n+1/6}\left(k_r\dfrac{d-c}{2}\right)}{(k_r a)^{1/6}\left(k_r\dfrac{d-c}{2}\right)^{1/6}} \tag{C.2}$$

where upper term is for even n, while the lower ones for odd m, while

$$H_{mn}^{(0)s} = H_{m,n+1}^{(1)s}\Big|_{\substack{\nu=0\\ \mu=k_0}}.$$

and

$$H_{mn}^{(0)a} = H_{m,n}^{(1)a}\Big|_{\substack{\nu=0\\ \mu=k_0}}.$$

$$Q_{mn}^{(1)s} = \frac{\mu\delta_0}{k_0\cosh^2 k_0 h}\left[2\sum_{r=1}^{\infty}\left\{\frac{2k_r}{s_r\delta_r}\begin{pmatrix}(-1)^{n/2}\cos k_r\left(h-\dfrac{c+d}{2}\right)\\ (-1)^{\frac{n-1}{2}}\sin k_r\left(h-\dfrac{c+d}{2}\right)\end{pmatrix}\right.\right.$$
$$\times\begin{pmatrix}(-1)^{m/2}\cos k_r\left(h-\dfrac{c+d}{2}\right)\\ (-1)^{\frac{m-1}{2}}\sin k_r\left(h-\dfrac{c+d}{2}\right)\end{pmatrix}\frac{J_{n+1/6}\left(k_r\dfrac{d-c}{2}\right)J_{m+1/6}\left(k_r\dfrac{d-c}{2}\right)}{\left(k_r\dfrac{d-c}{2}\right)^{1/3}} + \frac{\coth\xi_r b}{(d-c)\xi_r}\begin{pmatrix}(-1)^{m/2}\cos\dfrac{r\pi}{2}\\ (-1)^{\frac{n-1}{2}}\sin\dfrac{r\pi}{2}\end{pmatrix}$$
$$\left.\left.\times\begin{pmatrix}(-1)^{n/2}\cos\dfrac{r\pi}{2})\\ (-1)^{\frac{m-1}{2}}\sin\dfrac{r\pi}{2}\end{pmatrix}\frac{J_{n+1/6}\left(\dfrac{r\pi}{2}\right)J_{m+1/6}\left(\dfrac{r\pi}{2}\right)}{\left(\dfrac{r\pi}{2}\right)^{1/3}}\right\} + \frac{12\pi(2)^{1/3}}{(d-c)\{\Gamma(1/3)\}^4}\frac{\coth\nu b}{\nu}\delta_{0n}\delta_{0m}\right] \tag{C.3}$$

Here, also the upper terms are for even n, even m while the lower ones for odd n, odd m. $Q_{mn}^{(1)a}$ is obtained by replacing ''coth'' by ''tanh'' in (A.3).

$Q_{mn}^{(0)s}$ is obtained by taking $\nu = 0$, $\mu = k_0$, $n = n + 1$, $m = m + 1$ and deleting the term $[12\pi(2)^{1/3}\coth\nu b]\nu\delta_{0n}\delta_{0m}/[(d-c)\{\Gamma(1/3)\}^4]$ in the square bracket of Eq. (C.3) and

$$Q_{mn}^{(0)a} = \frac{\delta_0}{\cosh^2 k_0 h}\left[\sum_{r=1}^{\infty}\left\{\frac{4}{\delta_r}\begin{pmatrix}(-1)^{n/2}\cos k_r\left(h-\frac{c+d}{2}\right)\\(-1)^{\frac{n-1}{2}}\sin k_r\left(h-\frac{c+d}{2}\right)\end{pmatrix}\right.\right.$$

$$\times\begin{pmatrix}(-1)^{m/2}\cos k_r\left(h-\frac{c+d}{2}\right)\\(-1)^{\frac{m-1}{2}}\sin k_r\left(h-\frac{c+d}{2}\right)\end{pmatrix}\frac{J_{n+1/6}\left(k_r\frac{d-c}{2}\right)J_{m+1/6}\left(k_r\frac{d-c}{2}\right)}{\left(k_r\frac{d-c}{2}\right)^{1/3}}+\frac{\tanh\frac{4\pi b}{d-c}}{\left(\frac{r\pi}{2}\right)^{4/3}}\begin{pmatrix}(-1)^{n/2}\cos\frac{r\pi}{2}\\(-1)^{\frac{n-1}{2}}\sin\frac{r\pi}{2}\end{pmatrix}$$

$$\left.\left.\times\begin{pmatrix}(-1)^{m/2}\cos\frac{r\pi}{2}\\(-1)^{\frac{m-1}{2}}\sin\frac{r\pi}{2}\end{pmatrix}J_{n+1/6}\left(\frac{r\pi}{2}\right)J_{m+1/6}\left(\frac{r\pi}{2}\right)\right\}+\frac{12\pi b}{(d-c)}\frac{2^{1/3}}{\{\Gamma(1/3)\}^4}\delta_{0n}\delta_{0m}\right] \tag{C.4}$$

The upper term are for even n, even m and lower ones for odd n, odd m.

$$p_m^{(1)s,a} = \frac{I_{2m+1/6}(k_0 a)}{(k_0 a)^{1/6}}$$

$$q_m^{(1)s,a} = \frac{(-1)^m e^{k_0(h-\frac{c+d}{2})}+e^{-k_0(h-\frac{c+d}{2})}}{2\cosh k_0 h}\frac{I_{m+1/6}\left(k_0\frac{d-c}{2}\right)}{\left(k_0\frac{d-c}{2}\right)^{1/6}} \tag{C.5}$$

$$\begin{aligned}p_m^{(0)s,a} &= p_m^{(1)s,a}\\ q_m^{(0)s} &= q_{m+1}^{(1)s}\\ q_m^{(0)a} &= q_m^{(1)a}\end{aligned} \tag{C.6}$$

References

[1] Packham BA, Williams WE. A note on the transmission of water waves through small apertures. J. Inst. Maths Applies 1972;10:176–184.

[2] Losada MA, Losada IJ, Roldán AJ. Propagation of oblique incident waves past rigid vertical thin barriers. Appl. Ocean Res. 1992;14:191–199.

[3] Mandal BN, Dolai DP. Oblique water wave diffraction by thin vertical barriers in water of uniform finite depth. Appl. Ocean Res. 1994;16:195–203.

[4] Kanoria M, Mandal BN. Oblique wave diffraction by two parallel vertical barriers with submerged gaps in water of uniform finite depth. J. Tech. Phys. 1996;37:187–204.

[5] Banerjea S, Kanoria M, Dolai DP, Mandal BN. Oblique wave scattering by a submerged thin wall with gap in finite depth water. Appl. Ocean. Res. 1996;18:319–327.

[6] Das Pulak, Dolai DP, Mandal BN. Oblique water wave diffraction by two parallel thin barriers with gaps. J. Wtry. Port, Coastal and Ocean Engng. 1997;123:163–171.

[7] Mei CC, Black JL. Scattering of surface waves by rectangular obstacle in water of finite depth. J. Fluid Mech. 1969;38:499–511.

[8] Bai KJ. Diffraction of oblique waves by a infinite cylinder. J. Fluid Mech. 1975;68:513–535.

[9] Liu PL-F, Wu J. Wave transmission through submerged apertures. J. Wtry, Port, Coast and Ocean Engng. 1987;113:660–671.

[10] Evans DV, Fernyhough M. Edge waves along periodic coast lines, Part 2. J. Fluid Mech. 1995;297:307–325.

[11] Porter R, Evans DV. Complementary approximations to wave scattering by vertical barriers. J. Fluid Mech. 1995;294:155–180.

[12] Martin PA, Dalrymple RA. Scattering of long waves by cylindrical obstacles and gratings using matched asymptotic expansions. J. Fluid Mech. 1988;188:465–490.

[13] McIver P. Low frequency asymptotics of hydrodynamic forces on fixed and floating structures. In: Rahman M, editor. Ocean Wave Engineering, UK: Computational Mechanics Publications, 1994. pp. 1–49.

[14] Mandal BN, Kanoria M. Oblique wave scattering by thick barriers., Proceedings of 17th International Conference on Offshore Mechanics and Arctic Engineering, ASME, Lisbon, Portugal, July 1998 (Accepted for publication).

[15] Kanoria M, Dolai DP, Mandal BN. Water wave scattering by thick vertical barriers., J. Engng Math., in press.